# 1 Charge Estimates

We found the distribution of mostly likely experimental net charges for a population of the drops jumped in low-gravity. A covariance plot of the model variables is shown in Figure 1. The multicollinear dependence of charge on drop surface area, $A$, and the characteristic electric field, $E_0$, is evident. Assuming the main effect is the interaction between charge and electric field, a Robust Least Squares model fit $q \sim kAE_0$ (using the Python `statsmodels.formula.api.RLM` function), with the non-linear transformation $A = V_d^{2/3}$, found that $k = 5.01 \times 10^{-11} \pm 2.85 \times 10^{-11}$ with $R^2 = 0.946$. This model uses Huber's T norm, median absolute scaling, and H1 covariance estimation. A contour plot showing the estimated drop free charge as a function of $V_d$ and $\varphi_s$ is shown in Figure 2.

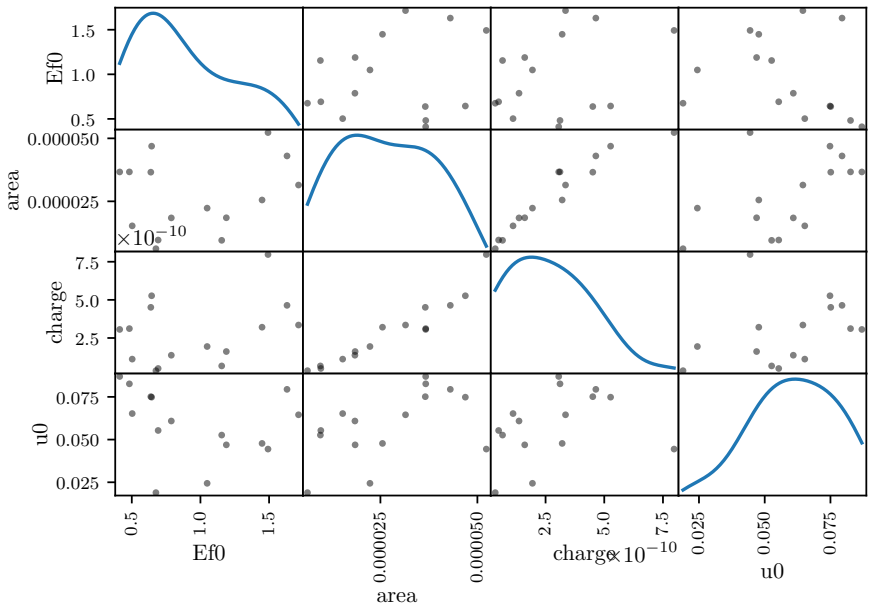


Figure 1: Covariance plot of main parameters $E_0$, $U_0$, droplet area ($V_d^{2/3}$), and $q$.

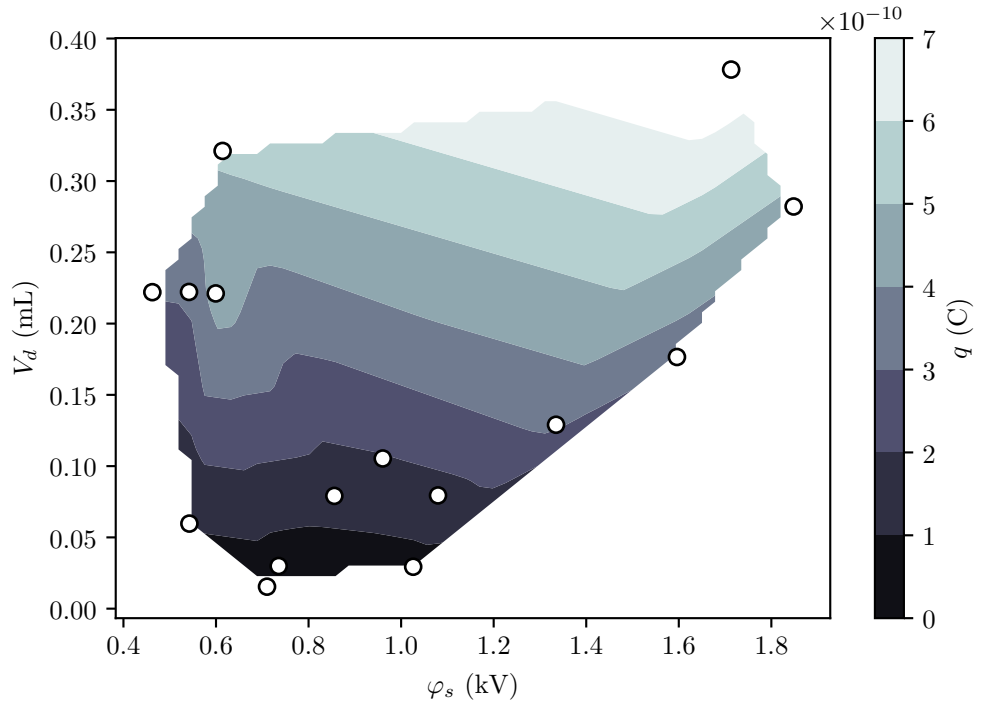


Figure 2: Charge $q$, as a function of $V_d$, $\varphi_s$.

A two-ways T-test comparison of charge distributions between the drop bounce experiment and a corollary experiment with zero electric field at the time of drop deposition on the superhydrophobic surface suggests that the drop charge is induced by the electric field, rather than through contact charging on the PTFE layer ($t = 5.11, p = 0.0002$). The T-test informs us that the charge distribution are about 5 times more different from each other as they are within each other, and there is a 0.02% probability that this result happened by chance. This corollary experiment is documented in Appendix **??**.

The model $q \sim kAE_0$ is incidentally very similar to the classical solution for the surface charge density of a half-spherical conductor with a field-induced

dipole [1]

$$\begin{aligned} q &= 3\epsilon_0 E_0 \int_A \cos\theta dA \\ &= 3\pi^{1/3} 6 \left(6V_d\right)^{2/3} \epsilon_0 E_0 \int_{\pi/2}^{4\pi/2} \cos\theta d\theta \\ &= k E_0 V_d^{2/3} \end{aligned}$$

with $k \approx 1.3 \times 10^{-10}$. This is also of a similar form to the charge found by Takamatsu and coauthors for drops falling from a grounded nozzle in an external electric field [2]

$$q = 4\pi\epsilon_0 \beta E_0 R_d^2$$

with $\beta \approx 2.63$.

## 2 Scale Quantities

The dielectrophoretic force plays a very small role when drops have net charge in a DC field; the condition to neglect the DEP force was satisfied for all experiments in the dataset. Dimensional drop apoapses scale closely with $\mathbb{E}\mathrm{u}$ as seen in Figure 3. The relative magnitudes of the simulated forces felt by the drops is shown in Figure 4. Forces acting on the drops vary in magnitude between $\mathcal{O}(10^{-6})$-$\mathcal{O}(10^{-4})$ N. We see that, of the drops in the experimental dataset only the two with the largest $\mathbb{E}\mathrm{u}$, $\mathbb{E}\mathrm{u} \sim \mathcal{O}(1)$ could appropriately be said to be in the inertial electro-viscous regime. In all other cases image forces are much stronger than drag. For these drops $\mathbb{E}\mathrm{u} \gg 1/8\pi$, and are likely on escape trajectories. The image forces themselves rapidly become small compared to Coulomb forces for drops with apoapses $\max(y) \gtrapprox L$, thus it is reasonable to claim that for intermediate drops Coulomb force scales as inertia, and we can neglect the effects of drag and image forces.

In the non-dimensional trajectories with short-time scaling shown in Figure 5, we see that the trajectory apoapses are consistently $\mathcal{O}(1)$, but most trajecto-

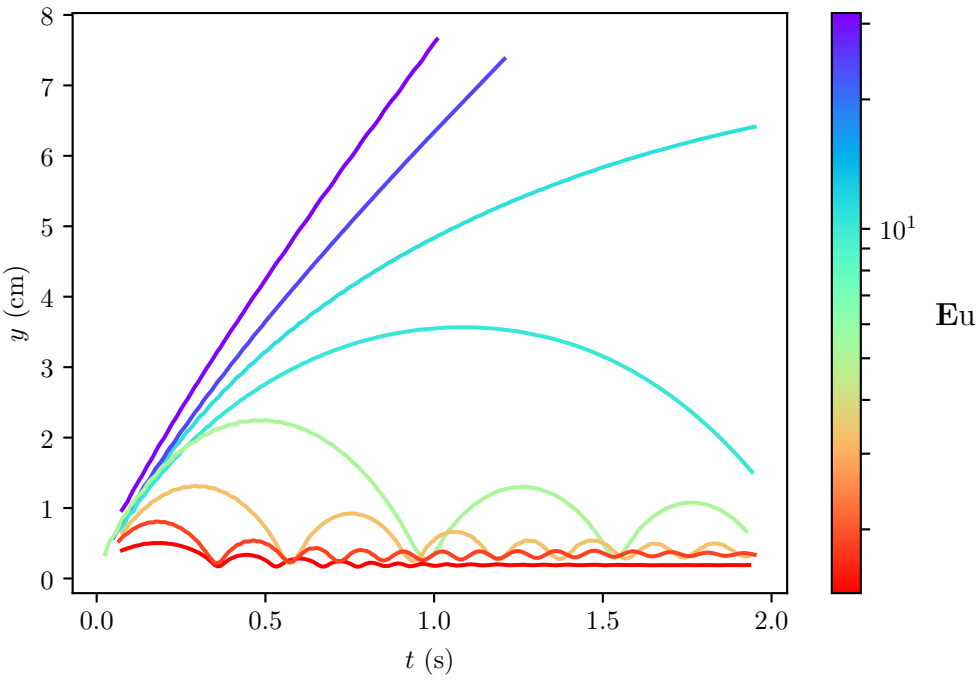


Figure 3: Drop trajectories as a function of $\mathbb{E}$u.

ries overshoot their characteristic time scale (which predicts returns at $\bar{t} = 2$ to the first order). We also observe that that $\mathbb{E}$u is not typically a small number in this regime, imperiling our use of asymptotic estimates in this regime. We can perhaps gain some insight by comparing the asymptotic estimate for return times to the scaled experimental return times. We see in Figure **??** that the long-time scaled non-dimensional time of first bounce in the experiment $t_b/t_c$, compares poorly to the asymptotic estimate for returns $t_f$ in the limit of small $\mathbb{E}\mathrm{u}_+$, this is due to the use on long-time scaling for drops with $y/L \ll 1$.

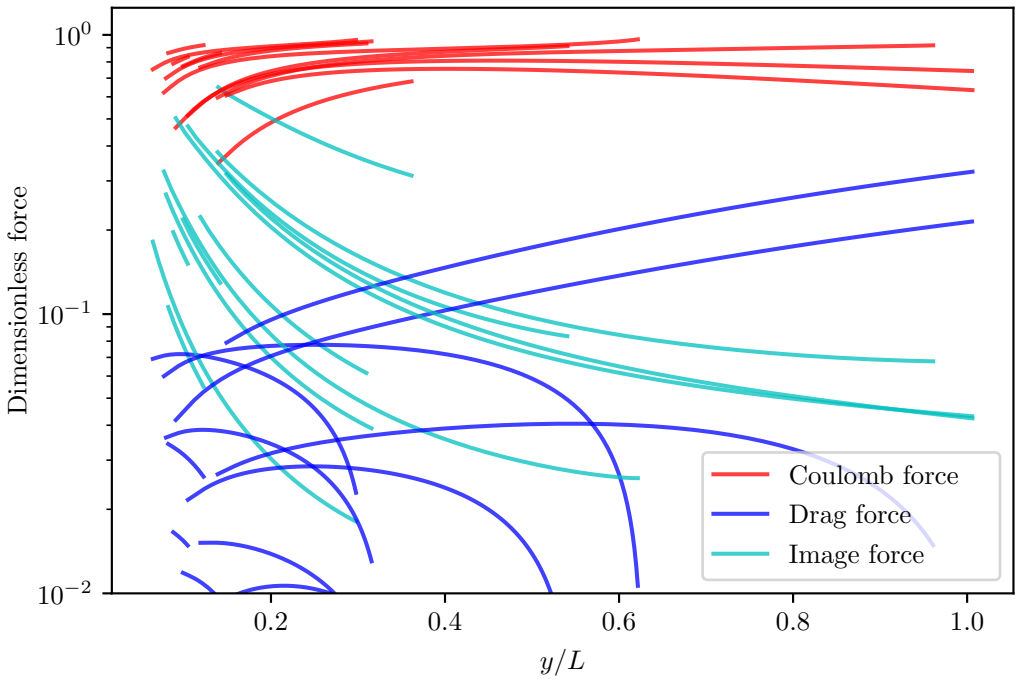


Figure 4: Simulated forces acting on the drop. Experiments are shown by order of increasing apoapse.

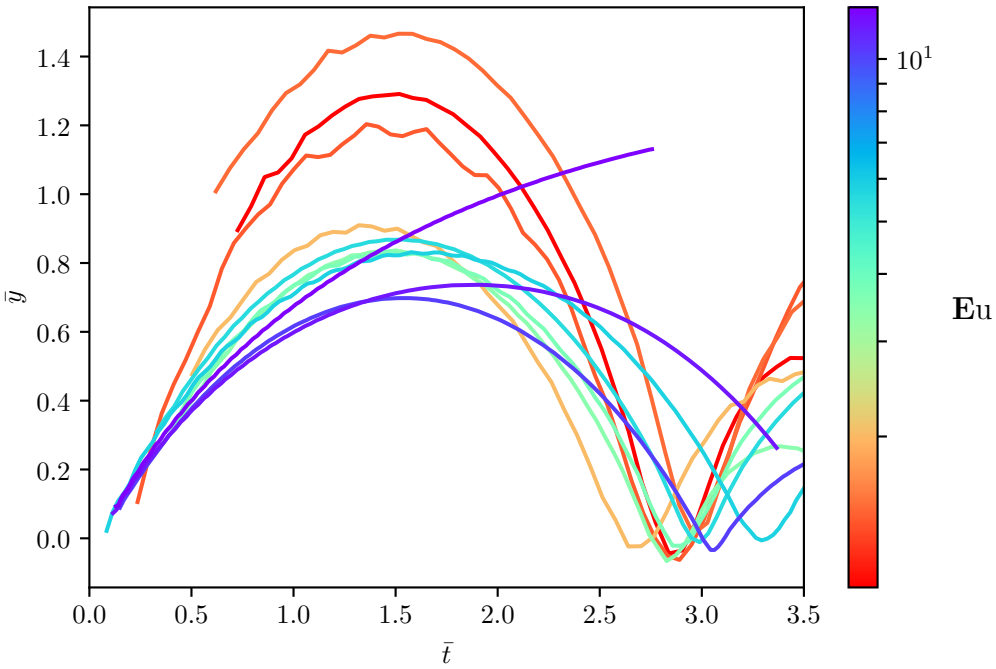


Figure 5: Non-dimensional trajectories with the short-time scaling.

The covariance of $\mathbb{I}$m with $\mathbb{E}$u is shown in Figure 6. Predictably, there is quite strong correlation between the dimensionless groups. We also see that $\mathbb{I}\text{m} < 1$ for all drops. Using an OLS regression, we find the model $\mathbb{I}\text{m} \sim (0.012 \pm 0.003)\mathbb{E}\text{u} + (0.212 \pm 0.036)$ with $R^2 = 0.59$.

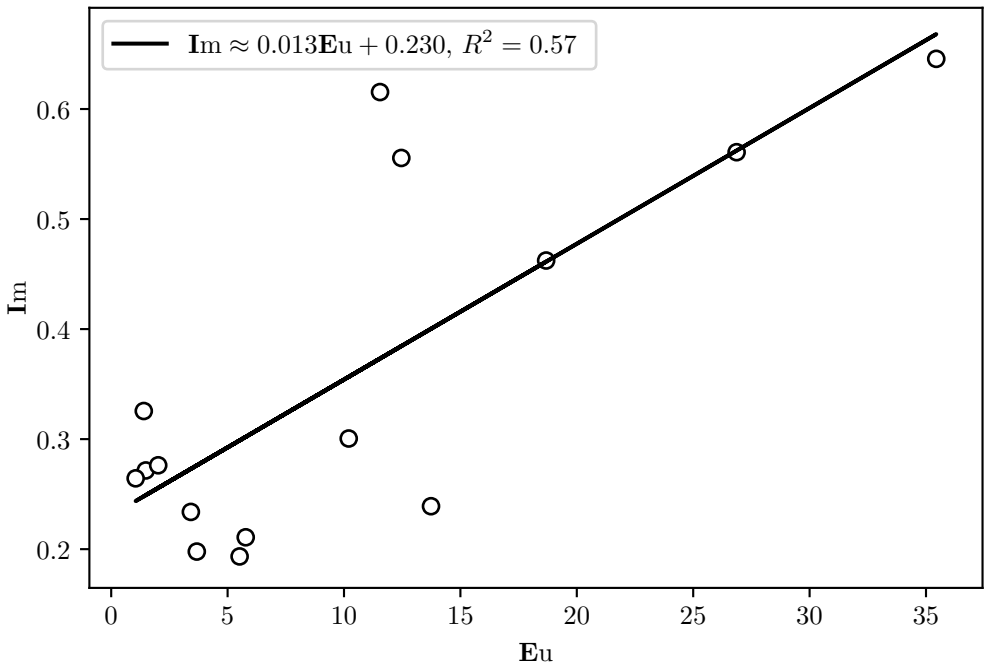


Figure 6: Experimental covariance between $\mathbb{E}$u and $\mathbb{I}$m.

We should note that there are several kinds of systematic error that influence our data. We assume that drop translate purely along the central axis of the electric field, but in practice, despite the improvement in surface charge density uniformity produced by corona charging, there are still local areas of especially high charge density. In principle, this kind of error should become small for drops which are far enough away from the charge distribution, that the geometry of the charge distribution disappears, and the electric field looks like that due to a point charge. Another form of error is in the initial velocity as it appears in $\mathbb{E}$u. Because we usually lose the first few frames of video due to camera shake transients at the start of the low-gravity experiment, we will consistently

underestimate $U_0$ because the drop will already have decelerated significantly during that period of time. The primary sources of random error are the effect of contact line hysteresis on the drop initial velocity, and of the variance in the MLE parameter estimates.

# 3 Impact Dynamics

Check the Oh numbers. Very little work to date on drop impacts outside of two regimes: first, very low $\mathbb{R}$e viscous drop spreading driven by capillary forces at the contact line, and second, impacts at "high" $\mathbb{W}$e. There has been some computational work with impacts at $\mathbb{R}\text{e} = 1.4$ (Fukai *et al.*), but the results are suspect as the model neglects uncompensated Young's force at the contact line (which is the dominant spreading force for low $\mathbb{R}$e impacts). Of course models for dynamic contact lines in general remain controversial, even for ordinary spreading of liquids, despite decades of work in the area.

Naivly neglecting dimensionless groups governing the dynamic contact line, the pertinent dimensionless groups for isothermal droplet impacts are the Weber number $\mathbb{W}\text{e} = \frac{\rho U^2 R_d}{\sigma}$, which is a ratio of droplet inertia to surface tension, the Ohnesorge number, $\mathbb{O}\text{h} = \frac{\mu}{\sqrt{\rho \sigma R_d}}$, which is a ratio of viscous to inertial and surface tension forces, and the Bond number, $\mathbb{B}$o, defined previously. The dynamics of spreading are characterized primarily by $\mathbb{W}$e and $\mathbb{O}$h. Additionally the final stages of spreading depend strongly on $\theta_e$, which is the static contact angle. The Weber number scales the *driving force* of the impact. In the more familiar case of high $\mathbb{W}$e the drop liquid bulk is driven radially outward by the impact induced pressure gradient, whereas in the case of small $\mathbb{W}$e the liquid is pulled outwards by capillary force (e.g. uncompensated Young's force) at the contact line. The Ohnesorge number, by contrast, scales the force that *resists* spreading. For large $\mathbb{O}$h the resistive force is viscous, whereas for low $\mathbb{O}$h the force is inertia.

We observe average drop impact $\mathbb{O}\text{h} \approx 2.18 \pm 0.36$, and $\mathbb{W}\text{e} \approx 0.28 \pm 0.22$.

Thus impact velocity plays little role in the spreading dynamics of the bounces, and viscous effects are important but do not dominate inertia. Notably we observe underdamped oscillations of drop interfaces during impact. according to (Schiaffino, 1997) viscous forces play a role in the final (which? describe) stage of spreading even for drop impact at very low $\mathbb{O}$h. In the regime of intermediate viscosity, following spreading the oscillations of the interface are damped with a characteristic time that is generally longer than the spreading time (again, given by $t_c \sim \left(\sigma/\rho R_d^3\right)^{1/2}$). The celebrated Hoffman-Tanner-Voinov law, which relates the contact line velocity $U_c$ of an isothermal spreading process to the static contact angle $\theta_e$ to the dynamic advancing contact angle $\theta_a$ by

$$\frac{\mu U_c}{\sigma} \approx \kappa \left(\theta_a^3 - \theta_e^3\right),$$

where $\kappa \approx 0.013$ is an empirical coefficient extracted from Hoffman's data. The Hoffman-Tanner-Voinov law implies that the transition between low $\mathbb{W}$e inviscid and viscous regimes occurs at $\mathbb{O}$h $\sim \mathcal{O}(10^{-2})$ rather than $\mathbb{O}$h $\sim \mathcal{O}(1)$ given by a naive scaling.

Some notes:

- **Schiaffino, 1997**